



Development of Multi-Walled Carbon Nanotube-Integrated Recycled Polyethylene Terephthalate Electrospun Antibacterial Face Mask

Md. Enamul Hoque^{1*}, Mirajul Alam Sarker², Md. Rubel Alam³ and Md. Abdul Gafur⁴

^{1,2} Department of Biomedical Engineering, Military Institute of Science and Technology (MIST), Dhaka, Bangladesh

³ Department of Knitwear Engineering, BGMEA University of Fashion and Technology (BUFT), Dhaka, Bangladesh

⁴ Bangladesh Council of Scientific and Industrial Research (BCSIR), Dhaka, Bangladesh

Abstract

In this study, electrospun nanofiber membranes were successfully fabricated by modifying recycled polyethylene terephthalate (r-PET) with multi-walled carbon nanotubes (MWCNTs) for face mask applications. The recycling of PET bottles ensures effective waste management, while the electrospinning process facilitates the creation of delicate nano-range fibers. The inclusion of MWCNTs aimed to assess the antibacterial activity of the resulting nanomembranes. The fabricated samples underwent comprehensive characterization, including scanning electron microscopy (SEM), ultimate tensile testing, particulate filtration efficiency (PFE) testing, Fourier transform infrared spectroscopy (FTIR), and antibacterial sensitivity assays, revealing significant findings. MWCNTs incorporation led to minor bead formation in the membranes, with fiber diameters ranging from 446 to 862 nm. However, MWCNTs resulted in reduced stiffness and tensile properties due to the disruption of polymer chain alignment. The nanofiber membranes demonstrated effective filtration of 0.3 μm particulates, achieving filtration rates between 96 to 97%. Functional group analysis confirmed the presence of both r-PET and MWCNTs in the composites. Although the r-PET/MWCNTs 12 kV membrane lacked an antibacterial zone of inhibition, it exhibited reductions of 28.64% for *S. aureus* and 31.9% for *E. coli*. These results collectively underscore the potential of r-PET/MWCNTs samples as an alternative nanofibrous membrane material for face masks.

Received: 30.04.2023

Revised: 05.05.2023

Accepted: 10.05.2023

Keywords: MWCNTs, r-PET, Electrospinning, Face Mask, Covid-19

Introduction

The COVID-19 pandemic has highlighted the importance of personal protective equipment (PPE), including face masks, in preventing the spread of infectious diseases (Humphreys, 2020; Martinelli et al., 2021; Rahman et al., 2022). Surgical masks are commonly used as PPE, consisting of layers of non-woven materials, including polypropylene, that filters out airborne particles (Adanur & Jayswal, 2022; Aragaw, 2020). However, the increased demand for face masks has led to shortages of

materials and rising costs, necessitating the search for alternative, sustainable materials that can be used in their manufacture.

Carbon nanotubes (CNTs) have a wide range of applications due to their remarkable physicochemical unique properties, such as chemical stability, mechanical strength, high electrical conductivity, optical, antibacterial, and thermal properties (Popov, 2004). CNTs have a wide range of possible uses, including composite

*Corresponding author e-mail: enamul1973@gmail.com; enamul1973@bme.mist.ac.bd

materials science, energy storage, electronics, the medical area, water purification, catalysis, and biotechnology (Venkataraman et al., 2019). CNTs have also gained interest as an antibacterial agent due to their potential in medical instruments (Teixeira-Santos et al., 2020).

On the other hand, recycled polyethylene terephthalate (r-PET) assumes a crucial role emblematic of sustainability and environmental responsibility. Annually, the world generates approximately 380 million tons of plastic, with PET constituting a significant portion of this waste. By repurposing r-PET in mask fabrication, a substantial environmental impact can be made, diverting a huge amount of PET waste from landfills. This recycling initiative not only reduces waste but also conserves energy, requiring 50-70% less energy compared to manufacturing virgin PET (Sarda et al., 2022). PET flake recycling has been projected to yield a net reduction in greenhouse gas emissions by approximately 1.8 tons of CO₂ equivalent per ton of recycled PET flake. Comparatively, the greenhouse gas emissions from recycled PET flakes, predominantly through mechanical recycling methods, are estimated to be 72% lower than those stemming from virgin PET flakes (Bataineh, 2020). The adoption of r-PET represents a paradigm shift towards a circular economy, minimizing the environmental footprint of personal protective equipment. Meanwhile, the electrospun nanofibrous membrane, known for its high surface area-to-volume ratio, serves as the mask's structural foundation, offering enhanced breathability and filtration efficiency (Hoque et al., 2023). However, electrospinning, while facilitating the creation of intricate membranes, also demands cautious consideration of its energy consumption and waste output.

In this study, we developed an antibacterial face mask using multi-walled carbon nanotubes (MWCNTs) integrated r-PET electrospun nanofibrous membranes. MWCNTs have been

extensively studied for their antibacterial properties, which are attributed to their large surface area and high aspect ratio, allowing them to pierce bacterial cell membranes and disrupt their function (Saleemi et al., 2022). The use of r-PET in electrospinning has been explored due to its desirable mechanical properties and sustainability, making it an attractive alternative to traditional materials (Bonfim et al., 2021).

Our objective was to develop an alternative material for the middle layers of surgical masks that is both sustainable and effective in preventing the spread of bacteria. The developed face mask was evaluated against *Staphylococcus aureus* and *Escherichia coli* to assess its antibacterial efficacy.

In this paper, we describe the materials and methods used to fabricate the MWCNTs integrated r-PET electrospun nanofibrous membrane, as well as the characterization of the resulting face mask. We also discussed the antibacterial properties of the face mask and its potential as a sustainable alternative to traditional surgical masks.

Materials and methods

Materials

r-PET was obtained from commercially available water bottles at different stores in Bangladesh and further purification was done prior to utilization. Trifluoroacetic acid (TFA) from Research-Lab Fine Chem Industries (Mumbai, India), and dichloromethane from MERK (Germany) were purchased from local vendors. MWCNTs were obtained from XFNano (China). The average diameter of CNT was 50 nm and the average length was 10-20 μ m.

Solution preparation

Water bottles made of PET were collected and cleaned using detergent and distilled water. Subsequently, they were cut into small square-shaped flakes, with an average size of 10 \times 10 mm. The PET chips were then rinsed with methanol and deionized water, followed by sun drying. To create

the r-PET solution, 15 wt.% (w/w) of PET flakes were weighed and mixed with TFA and dichloromethane (DCM) in a 1:3 ratio within an airtight conical flask with a screw cap. The solution was stirred for 1 hour using a magnetic stirrer at room temperature. For the r-PET/MWCNTs solution, 0.5 wt.% (w/w) of MWCNTs was added to the r-PET solution. The mixture was stirred for an additional 1 hour with a magnetic stirrer and then sonicated for 1 hour in an ultrasonic water bath. Finally, the solution was stirred again for 1 hour without the application of heat.

Fabrication of nanofibers

Utilizing a Nano Fiber Electrospinning Unit (Model no: HO-NFES-040; Holmarc, India), the nanofibrous membrane for the face mask was produced. Two distinct sample categories were established: (a) r-PET, and (b) r-PET/MWCNTs. Employing a 20 mL syringe, 5 mL of solution was drawn in each instance. The needle tip-to-collector distance measured 100 mm, and the inner diameter of the needle was nominally 0.5 mm. The syringe pump bench's traverse motion was adjusted to 1 mm/sec. To generate three samples of each kind, voltage parameters of 8, 10, and 12 kV were applied. A constant flow rate of 0.8 mL/hr was maintained for all samples, resulting in electrospinning current fluctuating between 0 and 2 μ A. Despite occasional shutdowns for needle tip cleaning, the average production time per sample was upheld at 1 hour.

Optimization of electrospinning

In our study, we focused on fabricating samples using specific voltages (8, 10, and 12 kV) for each material, rather than extensively optimizing parameters like flow rate, voltage, distance, temperature, and viscosity. Our goal was to analyze sample antibacterial activity and potential for face mask production.

Solution flow rate optimization involved trial and adjustment. A computer controller simultaneously regulated flow rate and pump motion while maintaining a constant voltage. This allowed real-time adjustments without system shutdown. Handling volatile solvents posed a challenge; continuous flow adjustment ensured steady fiber flow and a well-formed Taylor cone. Fiber formation observation was aided by adjusted halogen light.

After fine-tuning, a flow rate of 0.8 mL/hr yielded consistent deposition and uninterrupted fiber formation. Rates below caused intermittent deposition and blockages; higher rates led to excess solution dropping from the needle tip due to gravity. Traverse motion was set at 1 mm/sec for smooth fiber formation.

The impact of chosen voltages on sample morphology is discussed in the subsequent morphology analysis section.

Fabrication of face mask

The face mask was fabricated using a four-layer sandwich structure, mimicking the design of existing surgical masks. The consecutive layers consisted of a hydrophobic non-woven polypropylene (PP) material as the outer layer, followed by a layer of melt-blown PP, an electrospun nanomaterial composed of recycled polyethylene terephthalate (r-PET) with multi-walled carbon nanotubes (MWCNTs), and finally, a hydrophilic non-woven PP as the inner layer (Figure 1). These layers were sequentially assembled and securely stitched together using a sewing machine, forming a mask with dimensions measuring 17.9 cm x 9.4 cm. Additionally, a flexible strip was integrated to ensure a secure fit around the nose, enhancing the mask's overall functionality and wearability.

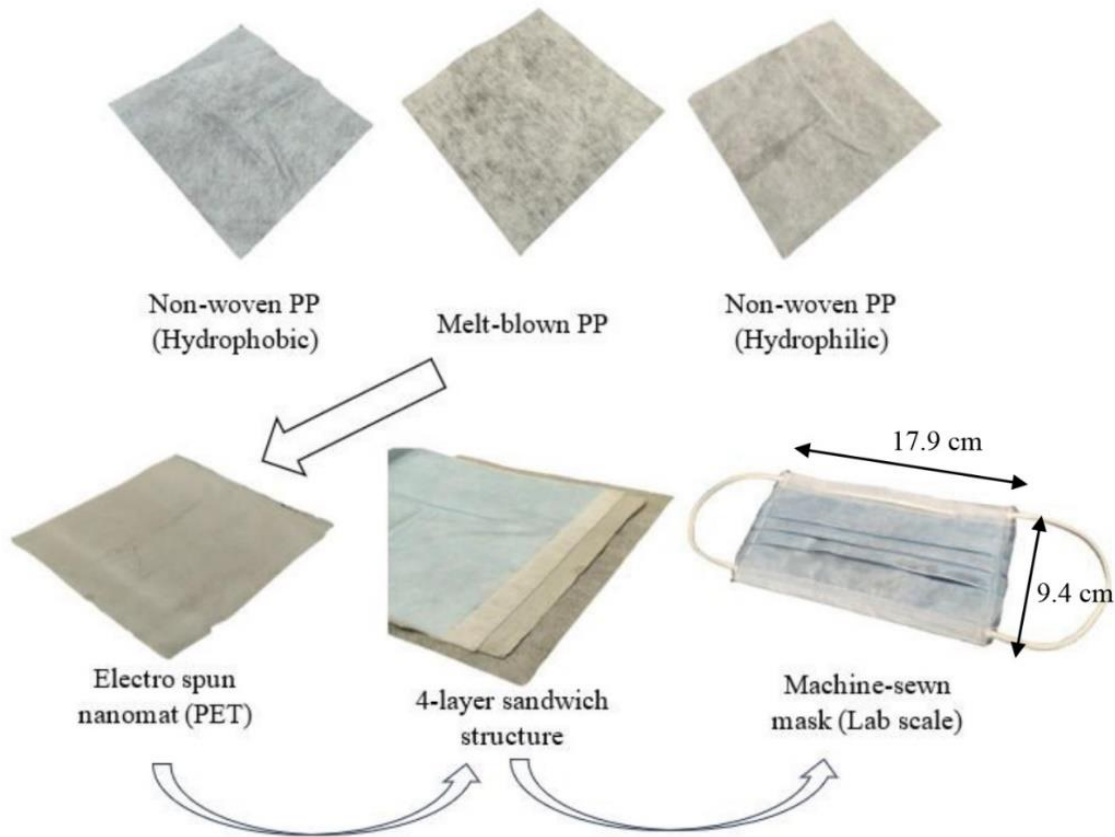


Figure 1. Fabrication process of the face mask

Characterization

SEM Analysis

The fiber morphology of r-PET and r-PET/MWCNTs nanofibers was observed using (SEM) (Vega 4 LMU; Tescan, Czech Republic). The SEM images were acquired to investigate the surface morphology of the fibers. Before analysis, all samples were sputter-coated with gold to ensure uniform surface conductivity.

SEM images of electrospun samples were processed using Adobe Photoshop and ImageJ software for fiber morphology analysis. Adobe Photoshop's color range tool masked pores in each sample and ImageJ measured the total pixel value of masked areas for porosity calculation. Additionally, ImageJ determined the average fiber diameter.

Ultimate Tensile Test

The mechanical properties of the electrospun membrane were studied using the Ultimate Tensile Test Machine model Z010, manufactured by Zwick Roell, Germany. The TestExpert software was used to operate the machine and collect data. Prior to testing, the specimen was mounted in a test window frame to ensure uniform stress distribution and prevent any unwanted stretching. A 500 N load cell was used to apply a tensile force to the specimen, and the test was performed following the ASTM standard D882. The specimen was gradually subjected to increasing loads until it eventually failed. The stress (σ), strain (ϵ), and Young's modulus (E) were calculated using standard equations,

$$\sigma = \frac{F}{A} \quad (1)$$

$$\varepsilon = \frac{\Delta l}{l} \quad (2)$$

$$E = \frac{\sigma}{\varepsilon} \quad (3)$$

where F (N) represents the applied force, A (m^2) the cross-sectional area of the specimen, and Δl (m) and l (m) are the change in length and original length of the specimen, respectively. The testing process was performed once to obtain reliable and reproducible results.

FTIR Spectroscopy Test

In this study, FTIR) was used to analyze the chemical composition and molecular structure of electrospun nanofibrous membranes. The FTIR analysis was conducted using a high-performance FTIR instrument (model: FT/IR-4700, JASCO Corporation, Japan). A sample of the material was prepared and placed on the instrument's sample holder, and a spectrum was generated by passing an infrared beam through the sample and measuring the amount of infrared radiation absorbed by the material. The obtained FTIR spectrum was analyzed to identify the functional groups present in the material, determine its chemical composition, and study its molecular structure.

PFE Test

To assess the particulate filtration efficiency (PFE) of the nanofibrous membrane in the face mask, a KANOMAX-3910 particle counter (Japan) was utilized. This device can detect particles of various sizes; however, for this evaluation, particles sized at $0.3 \mu\text{m}$ were used to mimic small airborne particles that could transmit respiratory infections. The PFE test determines the percentage of $0.3 \mu\text{m}$ particles filtered out by the mask material. During the test, a stream of $0.3 \mu\text{m}$ particles is directed through the face mask, and the particle count is measured both before and after filtration. This test followed the ASTM F2299 standard.

Antibacterial Test

The antimicrobial sensitivity of *E. coli* (ATCC:11775) and *Staphylococcus aureus* (ATCC:6538) to the electrospun nanofibrous membrane was evaluated using the Kirby-Bauer disk diffusion test. The samples were cut into $7 \text{ mm} \times 7 \text{ mm}$ pieces, and placed on agar plates inoculated with the bacteria at a concentration of 1.5×10^5 CFU/mL. After incubation, the diameter of the zones of inhibition (ZOI) around the squares was measured to assess the sample's antimicrobial activity.

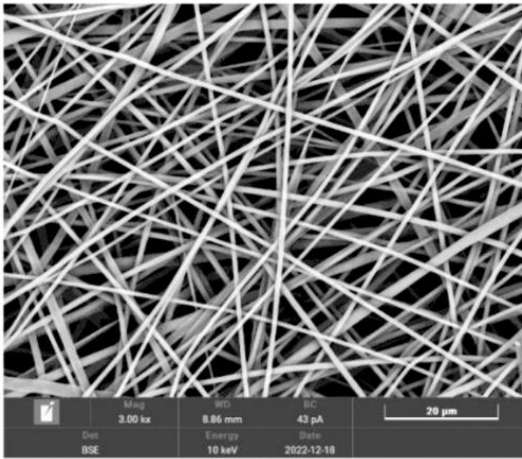
Results and Discussion

Morphology Analysis

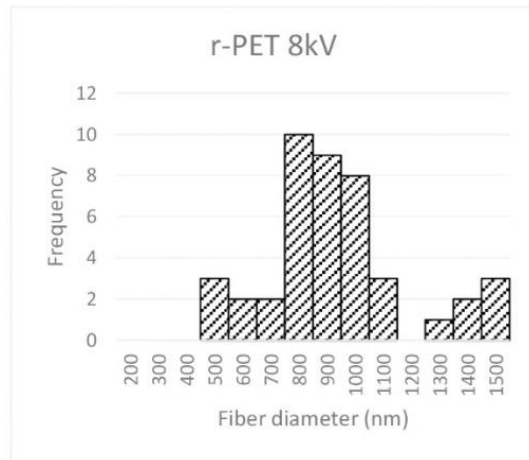
Porosity was measured by analyzing the SEM images with the help of 'ImageJ' and 'Adobe Photoshop' software and it revealed varied void spaces in electrospun samples. 8 kV r-PET sample demonstrated 6.5% porosity, suggesting enhanced breathability. 10 kV r-PET had 4.93% porosity, indicating denser structure. 12 kV r-PET had 4.04% porosity. The r-PET/MWCNTs samples showed porosity of 6.4, 5.22, and 4.55% for 8, 10, and 12 kV, respectively, with minor MWCNTs influence.

Fiber diameter investigation showed a decreasing trend with higher voltage. r-PET samples had diameters of 1006.68 nm (8 kV), 415 nm (10 kV), and 283.66 nm (12 kV). r-PET/MWCNTs samples exhibited diameters of 1153.9 nm, 639.9 nm, and 440.18 nm for corresponding voltages. Higher voltages yielded finer fibers due to increased stretching of the fibers (Haider et al., 2018). Incorporating MWCNTs caused occasional bead formation. Mode values were 827 nm (8 kV), 290 nm (10 kV), 243 nm (12 kV) for r-PET, and 862 nm, 671 nm, 446 nm for r-PET/MWCNTs. Both samples can be defined as nanomembranes based on the mode values (Figure 2).

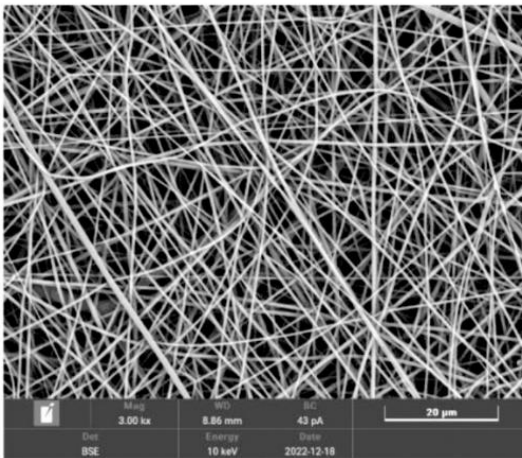
Fiber alignment displayed an overlapping cross pattern due to traverse motion of the syringe pump bench. r-PET fibers appeared finer than r-PET/MWCNTs, suggesting MWCNTs affected alignment.



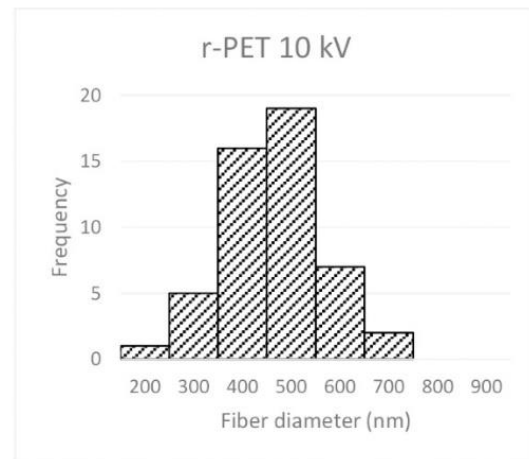
(c) r-PET 8 kV



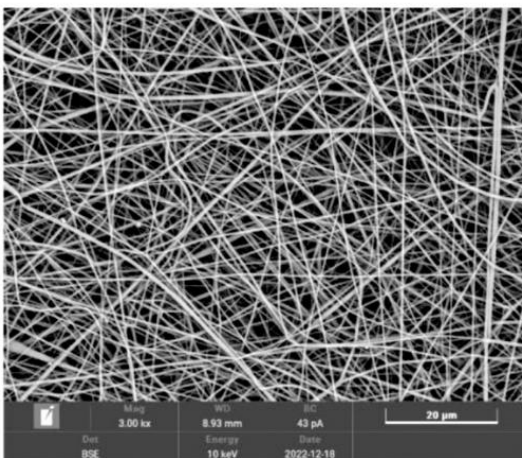
(iii)



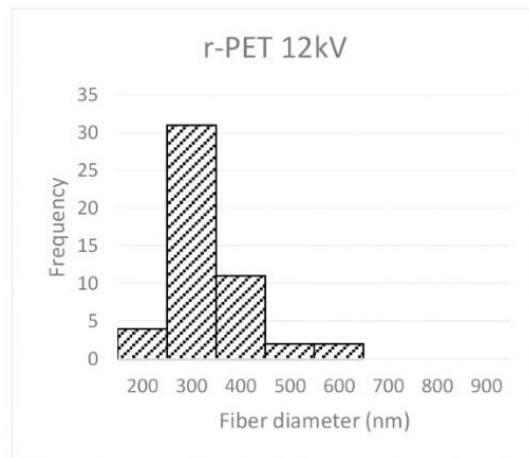
(c) r-PET 10 kV



(iii)

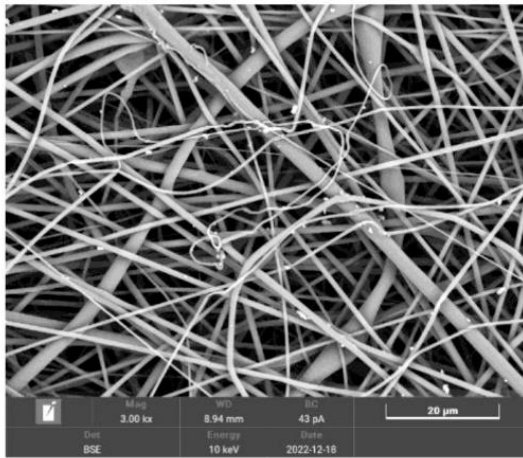
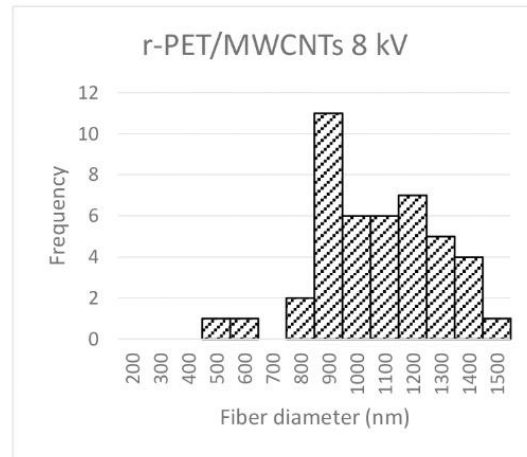


(c) r-PET 12 kV

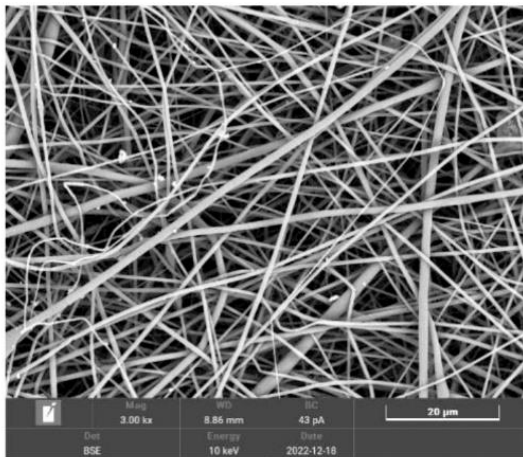
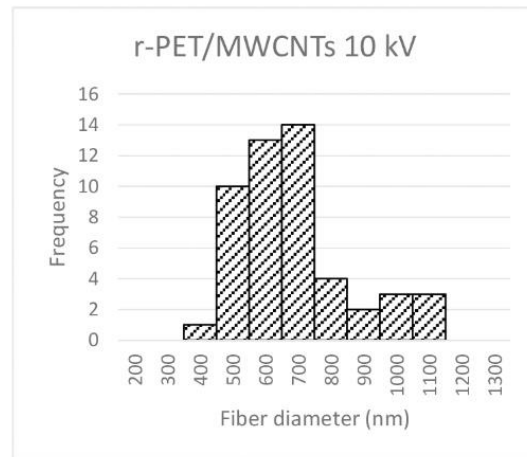


(iii)

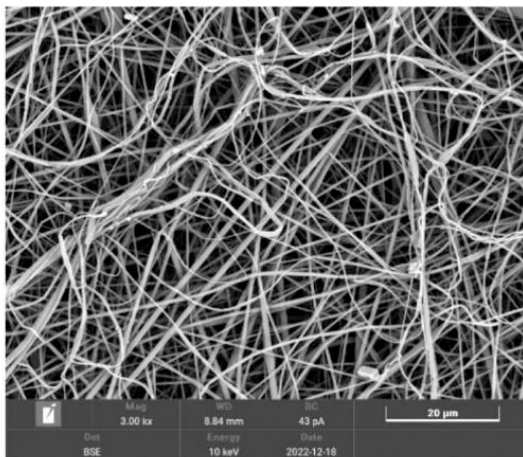
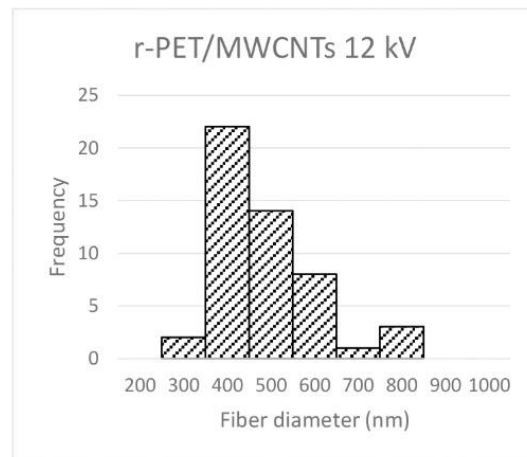
continued

(f) *r-PET/MWCNTs 8 kV*

(vi)

(f) *r-PET/MWCNTs 10 kV*

(vi)

(f) *r-PET/MWCNTs 12 kV*

(vi)

Figure 2. SEM Images and Histograms of r-PET and r-PET/MWCNTs samples fabricated at three different voltage levels. Histograms represent the frequency of fiber diameter for 50 randomly measured fibers within the SEM image samples.

FTIR Spectroscopic Analysis

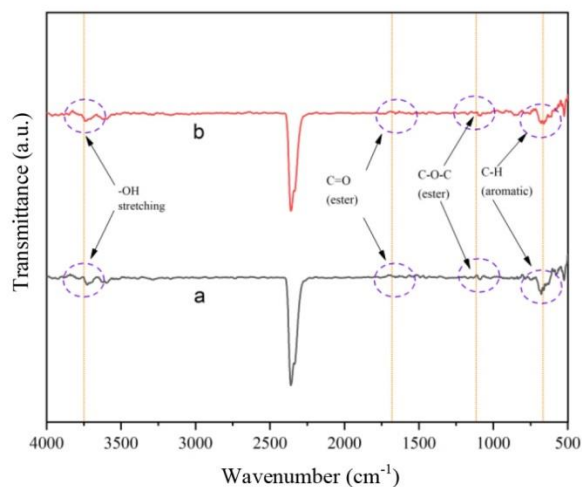


Figure 3. FTIR of (a) r-PET 10 kV and (b) r-PET/MWCNTs 10 kV nanofibers membranes.

Figure 3 illustrates the FTIR graph of r-PET 10 kV and r-PET/MWCNTs 10 kV fabricated electrospun nanofibers membrane. This analytical tool is used to identify the functional group of the fabricated samples. Both the membranes have the same transmittance peaks at different wave numbers. Since MWCNTs is a non-ionized group, so it cannot establish bonds with polyester fibers (Abubakre et al., 2023). The r-PET membrane exhibits a peak at 3726 cm^{-1} for the -OH group, which has been extended due to the development of weak hydrogen bonds in the r-PET/MWCNTs membrane (Mallakpour & Behranvand, 2016). In the membranes, the benzene ring has been detected as absorption peaks in the spectra at 1600-1700, 1100-1150, and $650\text{-}800\text{ cm}^{-1}$. The spectrum peaks corresponding to ester (C=O, C-O-C) and aromatic C-H bonds indicate the distinctive presence of the aromatic benzene ring within both the r-PET and MWCNTs. These spectral features collectively confirm the characteristic signatures of the aromatic benzene ring in both components.

Mechanical properties

The results obtained from the mechanical testing provide valuable insights into the properties of the electrospun samples at different applied voltages and with the incorporation of MWCNTs. Looking

at the tensile modulus at Figure 4b, we observe that the r-PET sample created at 10 kV exhibited the highest stiffness with a value of 113 MPa, followed by the r-PET sample at 8 kV with a tensile modulus of 79.2 MPa. On the other hand, the r-PET sample at 12 kV showed a lower tensile modulus of 48.3 MPa. This could be due to an optimal balance between polymer chain alignment and stretching during the electrospinning process. The electrostatic forces at 10 kV might have facilitated better molecular alignment, resulting in a more organized and aligned fiber structure. This enhanced alignment typically contributes to higher stiffness or tensile modulus in polymer materials (Baji et al., 2010). On the other hand, the addition of MWCNTs resulted in reduced tensile modulus values compared to pure r-PET samples. This is due to uneven dispersion or clustering of MWCNTs disrupted polymer chain alignment during electrospinning, weakening the material's stiffness. However, Inadequate bonding between MWCNTs and r-PET, as well as potential agglomeration, further contributed to reduced tensile modulus (Dai et al., 2016). Similarly, regarding tensile strength, both the r-PET and r-PET/MWCNTs samples at 10 kV showed the highest value of 4.74 MPa and 3.83 MPa (Figure 4a), suggesting that this voltage facilitated optimal chain alignment and stretching during fabrication.

Similar trends were observed for yield strength in Figure 4c, where the r-PET/MWCNTs sample at 10 kV displayed the highest value of 3.11 MPa, and the r-PET sample at 8 kV showed a yield strength of 2.72 MPa. The r-PET/MWCNTs sample at 12 kV had the lowest yield strength of 2.25 MPa. In terms of strain at break (Figure 4d), the r-PET sample at 8 kV demonstrated the highest value of 150%, indicating good ductility and the ability to undergo significant deformation before failure. The r-PET/MWCNTs samples showed slightly lower strain at break values, with the sample at 10 kV exhibiting 84% and the sample at 12 kV showing 90%. Overall, the data indicates that the applied voltage during electrospinning and the incorporation of MWCNTs significantly influenced the mechanical properties of the electrospun samples. Higher applied voltages generally led to improved stiffness but slightly reduced ductility. The addition of MWCNTs resulted in reduced

stiffness and tensile properties, likely due to the disruption of polymer chain alignment caused by the presence of nanotubes (Baji et al., 2010; Dai et al., 2016).

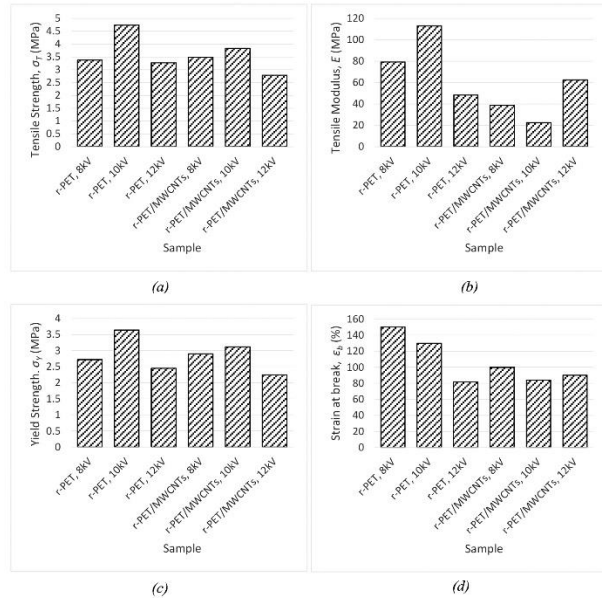


Figure 4. Histograms representing (a) Tensile strength, σ_T , (b) Tensile modulus, E , (c) Yield strength, σ_Y , (d) Strain at break, ϵ_b of the electrospun samples

Table 1. Mechanical properties of electrospun r-PET and r-PET/MWCNTs samples

Sample Name	Tensile Modulus, E (MPa)	Tensile Strength, σ_T (MPa)	Yield Strength, σ_Y (MPa)	Strain at Break, ϵ_b (%)
r-PET, 8 kV	79.2	3.37	2.72	150
r-PET, 10 kV	113	4.74	3.64	130
r-PET, 12 kV	48.3	3.27	2.45	82
r-PET/MWCNTs, 8 kV	38.7	3.49	2.90	100
r-PET/MWCNTs, 10 kV	22.4	3.83	3.11	84
r-PET/MWCNTs, 12 kV	62.5	2.78	2.25	90

Filtration Ability

The results from the particulate filtration assessment of the six electrospun samples demonstrate a strikingly consistent ability to remove 0.3 μm -sized particles from the air. The r-PET samples, exposed to varying voltage levels (8, 10, and 12 kV), displayed

average removal rates of 97.04 %, 96.88 %, and 96.03 %, respectively. Interestingly, the introduction of MWCNTs into the r-PET samples had an insignificant effect on filtration efficiency. The r-PET/MWCNTs samples at 8 kV, 10 kV, and 12 kV exhibited average removal rates of 96.28 %, 96.37 %, and 96.52 %, respectively. The minor divergence in efficiency values across all specimens suggests that the presence of MWCNTs had minimal influence on filtration efficiency for this particle size. It also implies that the voltages utilized in this study had a marginal impact on filtration performance for the specified particle size (Bortolassi et al., 2019). However, the consistently high efficiency levels surpassing 96% underscore the potential of these electrospun samples for effective particulate filtration applications, positioning them as promising contenders for various air purification and filtration needs, including applications like face masks.

Table 2. Particulate filtration efficiency of the electrospun samples

Particle size	Sample	Avg. upstream count	Avg. downstream count	Avg. efficiency, %
0.3 μm	r-PET 8 kV	28607288	848043	97.04
	r-PET 10 kV	28843577	898350	96.88
	r-PET 12 kV	28718952	1141409	96.03
	r-PET/MWCNTs 8kV	28816219	1073573	96.28
	r-PET/MWCNTs 10 kV	29072515	1056892	96.37
	r-PET/MWCNTs 12 kV	28802442	1002309	96.52

Nonetheless, it is important to recognize that introducing more substantial variations in voltage could potentially exert an impact on the filtration efficiency pattern. Elevated voltage levels might prompt higher electrospinning rates, consequently influencing fiber structure and porosity (Deitzel et al., 2001), which could consequently affect filtration efficiency. Thus, conducting additional experiments encompassing a broader spectrum of voltage values has the potential to provide deeper

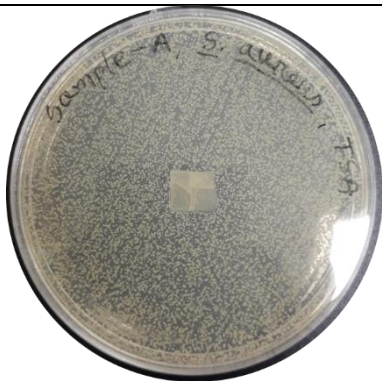
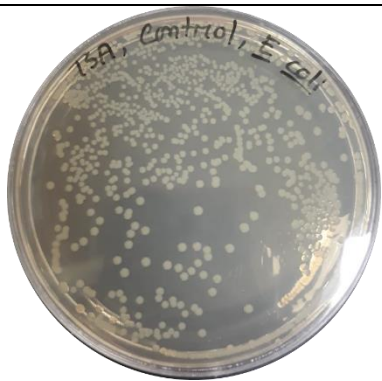
understanding regarding the correlation between voltage and filtration efficiency.

Antibacterial Sensitivity Analysis

Table 3 shows the antibacterial activity of fabricated nanofibers membrane. In this study, r-PET/MWCNTs for 12 kV membrane were tested against gram positive (*S. aureus*) and gram negative (*E. coli*) bacteria. Other membranes were not investigated because it is failed to demonstrate efficacy by ZOI. Because r-PET and MWCNTs are very insoluble in water, they do not come into touch with bacterial cells and so do not cause cell death. On the other hand, fabricated r-PET/MWCNTs for 12 kV membrane demonstrates greater bacterial reduction for gram positive bacteria than gram negative bacteria (despite the fact that both are inappropriate for creating ZOI). This is because the gram-positive cell wall is made up of linear ester

linkages that are cross-linked with short peptides from bacteria to produce a three-dimensional rigid structure (Navarre & Schneewind, 1999). A weak antibacterial property of MWCNTs has limited the applicability in infectious diseases in this cornerstone. To address this issue, antibiotics (Vancomycin hydrochloride, carboxymethylated chitosan) are used to treat severe but infectious bacterial (Varan et al., 2022) infections (Liu et al., 2017). Moreover, a meticulous approach is needed to disaggregate MWCNTs for improved antibacterial activities because they are hardly dispersed (Saleemi et al., 2020). For enhanced bacterial reduction percentage (99%), the electrospinning approach was utilized to successfully generate composite nanofibers from a solution of polyacrylonitrile (PAN), functionalized (f-MWCNTs), and silver nitrate (AgNO_3) in dimethylsulfoxide (Kizildag & Ucar, 2017).

Table 3. Antibacterial zone of inhibition assessment of fabricated nanofibers membrane

Particulars	<i>S. aureus</i>	<i>E. coli</i>
Agar disc of r-PET/MWCNTs, 12 kV		
ZOI	N/A	N/A
Reduction %	28.64*	31.9*

*Represents not suitable for the formation of zone

Conclusions

In this study, MWCNTs modified r-PET electrospun nanofibers membranes were successfully fabricated at different voltage for potential applications as face mask material. The nanofibers are continually produced and deposited on the collector at a very low flow rate (0.8

mL/hour). When flow rates were over this threshold, extra solution would sometimes fall from the needle tip due to gravity, depositing the entire solution droplet on the collector, whereas flow rates below this threshold resulted in intermittent fiber deposition and needle clogs. The porosity values of the r-PET/MWCNTs samples were 6.4, 5.22, and 4.55 % for 8, 10, and 12 kV, respectively, which are

extremely near to r-PET membranes. The addition of a small amount of MWCNTs had a minor effect on porosity, but it did not appreciably change the overall degree of porosity. Additionally, the incorporation of MWCNTs into the r-PET solution led to the formation of a small number of beads within the membranes and fibers diameter were 862 nm at 8 kV, 671 nm at 10 kV, and 446 nm at 12 kV. Moreover, MWCNTs resulted in reduced stiffness and tensile properties, likely due to the disruption of polymer chain alignment caused by the presence of nanotubes. The nanofibers membranes effectively filtrate the 0.3 μm particulate effectively 96-97 %. The 0.3 μm particle is efficiently filtrated at above 96% by the nanofiber membranes. Benzene ring, C-O-C, C=O, C-H functional groups have been identified which indicates the presence of r-PET and MWCNTs. Fabricated nanofibers membrane (r-PET/MWCNTs 12 kV) does not have an antibacterial zone of inhibition but reduces *S. aureus* and *E. coli* by 28.64 % and 31.9 %, respectively. Antibiotics may be introduced to the electrospun solution to increase its efficacy against microorganisms.

Acknowledgments

This research was funded by the Ministry of Science and Technology, Bangladesh (Grant ID No. EAS 450; 2021-2022). The authors would also like to thank the Military Institute of Science and Technology (MIST), BGMEA University of Fashion and Technology (BUFT), and the Bangladesh Council of Industrial and Scientific Research (BCSIR), for providing technical supports to this work.

Conflict of Interests

The authors have no conflict of interest.

Author Contribution Statement

MEH: Funding acquisition, supervision, conceptualization, review & editing, MAS: Conceptualization, investigation, methodology, formal analysis, data curation, writing original draft. MRA: Conceptualization, formal analysis, data curation, writing – review & editing. MAG: Lab facility, review & editing.

References

Abubakre, O. K., Medupin, R. O., Akintunde, I. B., Jimoh, O. T., Abdulkareem, A. S., Muriana, R. A., James, J. A., Ukoba, K. O., Jen, T.-C., & Yoro, K. O. (2023). Carbon nanotube-reinforced polymer

nanocomposites for sustainable biomedical applications: A review. *Journal of Science: Advanced Materials and Devices*, 8(2), 100557.

Adanur, S., & Jayswal, A. (2022). Filtration mechanisms and manufacturing methods of face masks: An overview. *Journal of Industrial Textiles*, 51(3), 3683S-3717S.

Aragaw, T. A. (2020). Surgical face masks as a potential source for microplastic pollution in the COVID-19 scenario. *Marine Pollution Bulletin*, 159, 111517.

Baji, A., Mai, Y.-W., Wong, S.-C., Abtahi, M., & Chen, P. (2010). Electrospinning of polymer nanofibers: Effects on oriented morphology, structures and tensile properties. *Composites Science and Technology*, 70(5), 703–718.

Bataineh, K. M. (2020). Life-Cycle Assessment of Recycling Postconsumer High-Density Polyethylene and Polyethylene Terephthalate. *Advances in Civil Engineering*, 2020, e8905431.

Bonfim, D. P. F., Cruz, F. G. S., Bretas, R. E. S., Guerra, V. G., & Aguiar, M. L. (2021). A Sustainable Recycling Alternative: Electrospun PET-Membranes for Air Nanofiltration. *Polymers*, 13(7), Article 7.

Bortolassi, A. C. C., Nagarajan, S., de Araújo Lima, B., Guerra, V. G., Aguiar, M. L., Huon, V., Soussan, L., Cornu, D., Miele, P., & Bechelany, M. (2019). Efficient nanoparticles removal and bactericidal action of electrospun nanofibers membranes for air filtration. *Materials Science and Engineering: C*, 102, 718–729.

Dai, L., Sun, J., Dai, L., & Sun, J. (2016). Mechanical Properties of Carbon Nanotubes-Polymer Composites. In *Carbon Nanotubes—Current Progress of their Polymer Composites*. IntechOpen.

Deitzel, J. M., Kleinmeyer, J., Harris, D., & Beck Tan, N. C. (2001). The effect of processing variables on the morphology of electrospun nanofibers and textiles. *Polymer*, 42(1), 261–272.

Haider, A., Haider, S., & Kang, I.-K. (2018). A comprehensive review summarizing the effect of electrospinning parameters and potential applications of nanofibers in biomedical and biotechnology. *Arabian Journal of Chemistry*, 11(8), 1165–1188.

Hoque, M. E., Sarker, M. A., Arif, K., Ali, M. A., & El-Bialy, T. (2023). Antibacterial/Antiviral Face Masks: Processing, Characteristics, Challenges, and Sustainability. *MIST INTERNATIONAL JOURNAL OF SCIENCE AND TECHNOLOGY*, 11, 61–79.

Humphreys, J. (2020). The importance of wearing masks in curtailing the COVID-19 pandemic. *Journal of*

- Family Medicine and Primary Care*, 9(6), 2606–2607.
- Kizildag, N., & Ucar, N. (2017). Investigation of the properties of PAN/f-MWCNTs/AgNPs composite nanofibers. *Journal of Industrial Textiles*, 47(2), 149–172.
- Liu, C., Shi, H., Yang, H., Yan, S., Luan, S., Li, Y., Teng, M., Khan, A. F., & Yin, J. (2017). Fabrication of antibacterial electrospun nanofibers with vancomycin-carbon nanotube via ultrasonication assistance. *Materials & Design*, 120, 128–134.
- Mallakpour, S., & Behranvand, V. (2016). Manufacture and characterization of nanocomposite materials obtained from incorporation of d-glucose functionalized MWCNTs into the recycled poly(ethylene terephthalate). *Designed Monomers and Polymers*, 19(4), 283–289.
- Martinelli, L., Kopilaš, V., Vidmar, M., Heavin, C., Machado, H., Todorović, Z., Buzas, N., Pot, M., Prainsack, B., & Gajović, S. (2021). Face Masks During the COVID-19 Pandemic: A Simple Protection Tool With Many Meanings. *Frontiers in Public Health*, 8.
- Navarre, W. W., & Schneewind, O. (1999). Surface Proteins of Gram-Positive Bacteria and Mechanisms of Their Targeting to the Cell Wall Envelope. *Microbiology and Molecular Biology Reviews*: MMBR, 63(1), 174–229.
- Popov, V. N. (2004). Carbon nanotubes: Properties and application. *Materials Science and Engineering: R: Reports*, 43(3), 61–102.
- Rahman, M. Z., Hoque, M. E., Alam, M. R., Rouf, M. A., Khan, S. I., Xu, H., & Ramakrishna, S. (2022). Face Masks to Combat Coronavirus (COVID-19)—Processing, Roles, Requirements, Efficacy, Risk and Sustainability. *Polymers*, 14(7), Article 7.
- Saleemi, M. A., Kong, Y. L., Yong, P. V. C., & Wong, E. H. (2022). An Overview of Antimicrobial Properties of Carbon Nanotubes-Based Nanocomposites. *Advanced Pharmaceutical Bulletin*, 12(3), 449–465.
- Saleemi, M. A., Yong, P. V. C., & Wong, E. H. (2020). Investigation of antimicrobial activity and cytotoxicity of synthesized surfactant-modified carbon nanotubes/polyurethane electrospun nanofibers. *Nano-Structures & Nano-Objects*, 24, 100612.
- Sarda, P., Hanan, J. C., Lawrence, J. G., & Allahkarami, M. (2022). Sustainability performance of polyethylene terephthalate, clarifying challenges and opportunities. *Journal of Polymer Science*, 60(1), 7–31.
- Teixeira-Santos, R., Gomes, M., Gomes, L. C., & Mergulhão, F. J. (2020). Antimicrobial and anti-adhesive properties of carbon nanotube-based surfaces for medical applications: A systematic review. *iScience*, 24(1), 102001.
- Varan, N. Y., Altay, P., & Çaydamli, Y. (2022). Antimicrobial Properties of Highly Elastic Conductive Poly(ethylene terephthalate)/Multiwalled Carbon Nanotube Fabrics. *Journal of Industrial Textiles*, 52, 15280837221121960.
- Venkataraman, A., Amadi, E. V., Chen, Y., & Papadopoulos, C. (2019). Carbon Nanotube Assembly and Integration for Applications. *Nanoscale Research Letters*, 14(1), 220.